ESTIMATION OF SENSOR OFFSETS FOR A UAV PLATFORM USING TIEPOINTS ONLY

Cheolwook Kim[1], Pyeong-Chae Lim[1], Taejung Kim[2] *

[1] Image Engineering Research Centre, 3DLabs Co. Ltd, 56 Songdogwahak-ro, Korea - (ileen3, lpc314)@3dlabs.co.kr
[2] Dept. of Geoinformatic Engineering, Inha University, 100 Inha-ro, Korea – tezid@inha.ac.kr

KEY WORDS: Sensor offsets, Boresight angle, Lever-arm, Re-weighted least square, Misalignment, Mosaic image.

ABSTRACT:
In a UAV system, physical sensor offsets occur between an observation sensor and a GPS/IMU sensor which represents the position of UAV. The difference of angle between the GPS/IMU sensor's axis and the observation sensor's axis is referred to as boresight angle. The difference in physical position between the two is referred to as lever-arm. It is important to obtain accurate offset values in order to utilize UAVs in rapid mapping manner. Due to the sensor offsets, misalignment error can be caused when generating a mosaic image. Offset values can be measured by using extensive ground control points. However, this is very costly and time-consuming. In this study, we describe an estimation method for sensor offsets using tie-points and re-weighted least square estimation method. The proposed method consists of 5 steps. Firstly, a frame images for the target area were classified into image strips based on the kappa value of initial EOPs (Exterior Orientation Parameters), after which tie points were extracted between adjacent images. Secondly, strip bundle adjustment was performed to update initial EOPs using images with the same flight direction. Thirdly, tie-points between adjacent strips were extracted. Fourthly, block bundle adjustment was performed in all images, using all extracted tie-points. Finally, a mosaic image is generated using the EOPs value to which the estimated sensor offset is applied. From this study, we confirmed that the sensor offset of the platform could be estimated only with the tie-points extracted between adjacent images. And we confirmed that misalignment was adjusted when generating mosaic image. We expect that our research makes UAV system to be operated more fluently.

1. INTRODUCTION

UAVs (Unmanned Aerial Vehicles) are utilized more cost-effectively, compared to satellites, and aircrafts. Due to this advantage, the use of UAVs platform is increasing with various observation sensor such as digital camera, hyperspectral camera, and lidar etc. (Kim et al., 2022). Recently, in the field such as deep learning, or AI (Artificial Intelligence), a spectral image data acquired with the UAVs is utilized (Mittal, P et al., 2022). The data for analysis is required to have high-geometric accuracy. However, they inevitably contain various factor of errors.

In a UAV system, the mounted error is common source of errors (Keyetieu and Seube, 2019). It occurs between an observation sensor and a GPS/IMU sensors. In this paper, we are going to refer mounted error to sensor offsets. The difference of angle between the GPS/IMU sensor's axis and the observation sensor's axis is referred to as boresight angle. The difference of physical position between the two is referred to as lever-arm.

Due to the sensor offsets, misalignment error can be caused when generating a mosaic image (Li et al., 2019). Figure 1 shows the example of misalignment in mosaic image. It is important to obtain accurate sensor offset values in order to utilize UAVs in rapid mapping manner. There are generally two ways to obtain sensor offsets. One is to measuring the physical sensor offsets directly. It is a straight-forward method. However, it must pay a significant cost and time for measurement facility preparation. Another way to obtain sensor offsets is to estimate them using extensive GCPs (Ground Control Points) (Habib et al., 2018). This is a more common way to obtain sensor offsets. Observation equations are established using GCP data and optimal solutions are estimated through least-square based estimation methods. Since GCPs are actual observed data, the estimated sensor offsets can be considered as reliable values. They were used as true sensor offset values in this study. They can be estimated and applied to all of datasets acquired from the same platform. However, in these way, extensive GCP Survey should be always performed. The result of estimation is depended on the quality of GCPs. Post-processing must be performed to extract corresponding points for the GCP, even if GCPs are acquired well. It could be sometimes more time-consuming with high cost. In this study, we are going to use only tie-points between adjacent images for sensor offset estimation. This way is much more cost-effective compared to the GCP method because tie-points can be extracted from images without any field survey. We expect that the proposed method can be effectively used in many cases because the error caused by sensor offsets is consistent for each image.

For an estimation method, re-weight least square estimation was used in experiment. It considers the weight for the unknown parameters with constrained condition. An initial weight is assigned to each parameter for the estimation. From this process, update to initial value is acquired, and initial weight are re-calculated to find optimal solution. When it converges to a reasonable weight value through iterations, and then the value is considered as an optimal solution.

From this study, we aim to investigate whether sensor offsets can be estimated using only tie-points, and how close the values are to the true values. We also aim to check that misalignment for mosaic image be effectively removed from the estimated and adjusted sensor offsets.

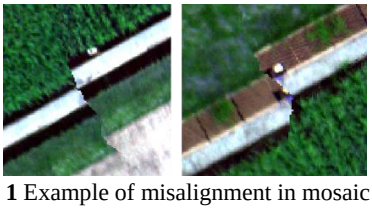

Figure 1 Example of misalignment in mosaic image.

* Corresponding author

2. MATERIALS AND METHODS

For experiments, we used 2 types of frame image datasets. Dataset 1 consisted of 52 UAV images taken over playground of KOPRI (Korea Polar Research Institute, Incheon). Dataset 2 consisted of 47 UAV images taken over NAAS (National Academy of Agricultural Sciences, Jeon-Ju). Figure 2 and 3 show the target area, and flight lines for Dataset 1 and 2, respectively. Flight lines for both datasets consisted of 4 lines. Line 1 and 3 were along the same flight direction and line 2 and 4 along the same flight direction opposite to that of line 1 and 2. Dataset 1 were observed at the altitude of 67m, and with flight speed of 3 m/sec. Dataset 2 were observed at the altitude of 90m, and with the flight speed of Dataset 1.

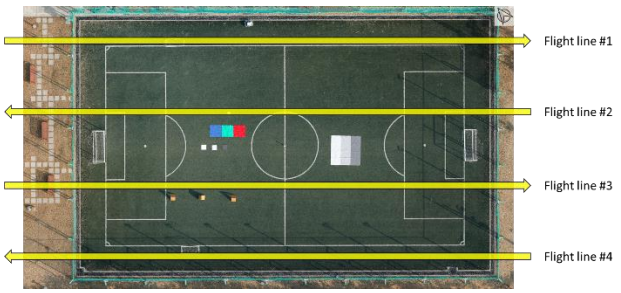

Figure 2. Target area in Dataset 1 (Korea Polar Research Institute, Incheon).

Figure 3. Target area in Dataset 2 (National Academy of Agricultural Sciences, Jeon-Ju).

Figure 4 shows the process of the proposed method. It consists of 5 steps. Firstly, a frame images for the target area were classified into image strips based on the kappa values of initial EOPs (Exterior Orientation Parameters), after which tie points were extracted between adjacent images. Secondly, strip bundle adjustment was performed to update initial EOPs using images with the same strip. Thirdly, tie-points between adjacent strips were extracted. Fourthly, block bundle adjustment was performed for all images, using all extracted tie-points. From following process, EOPs and sensor offsets are updated and estimated. Finally, a mosaic image is generated using the EOPs value to which the estimated sensor offsets are applied.

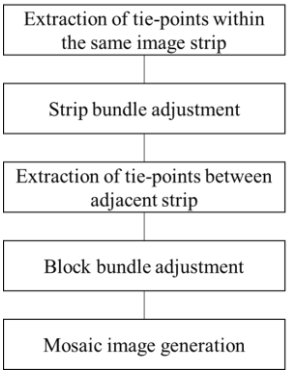

Figure 4. Flowchart of the proposed method.

2.1 Extraction of tie-points within the same image strip

We firstly classified each frame image into image strips. Each image had initial EOPs from the GPS/IMU sensor mounted on UAV platforms. We used kappa values of the EOPs to recognize image's flight direction. (Lim et al., 2021) Figure 5 explains the concept of forming image strips from kappa values. Images were classified into image strips. Each image strip consisted of images taken along the same flight direction. In these classified images, we attempted to extract tie-points. SURF (Speeded Up Robust Features) method was used to extract tie-points (Zhang et al., 2018). Only the feature points that were simultaneously observed in three adjacent images were selected and used as tie-points. In this paper, these points are referred to as triplets. The extracted triplets were used as data for strip bundle adjustment under collinearity conditions.

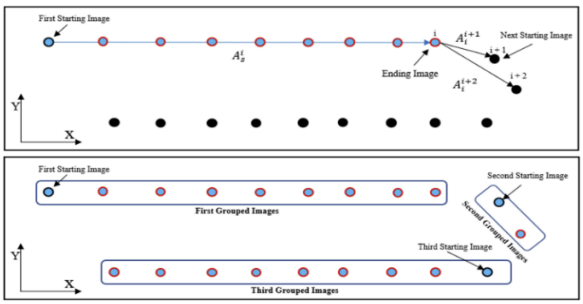

Figure 5. Concept of image separation for each strip (Lim et al., 2021)

2.2 Strip bundle adjustment

In this experiment, we used sensor model equations in Eq. 1. Eq. 1 describes a rotation matrix about the coordinate transformation from image space to ground space, based on the collinearity equation condition.

$$\begin{bmatrix} X_o \\ Y_o \\ Z_o \end{bmatrix} = \begin{bmatrix} X_s \\ Y_s \\ Z_s \end{bmatrix} + R_b^o \begin{bmatrix} X_L \\ Y_L \\ Z_L \end{bmatrix} + \lambda * R_i^o * R_i^i(w,p,k) * \begin{bmatrix} x_p \\ y_p \\ -f \end{bmatrix} \quad (1)$$

Where $x_p, y_p, -f$ = position vector for image and focal length
$R_i^i(w,p,k)$ = rotation matrix for boresight angle
R_i^o = rotation matrix from image space to object space
λ = scale factor
X_L, Y_L, Z_L = position vector for lever-arm of x, y, z
R_b^o = rotation matrix from body space to object space
X_s, Y_s, Z_s = position vector for platform (UAV)
X_o, Y_o, Z_o = position vector for geo-referenced points

$R_i^i(w,p,k)$, and X_L, Y_L, Z_L represent the unknown parameters that we want to estimate. However, in strip bundle adjustment, the unknown parameter is set to 0 and not used. It is estimated afterwards in the block bundle adjustment step. The tie-points extracted in 2.1 was substituted into Eq. 1, and strip bundle adjustment was performed for each strip (Figure 6). Through this process, we obtained the adjusted initial EOP, and adjusted tie-points. These were used in block bundle adjustment as initial values.

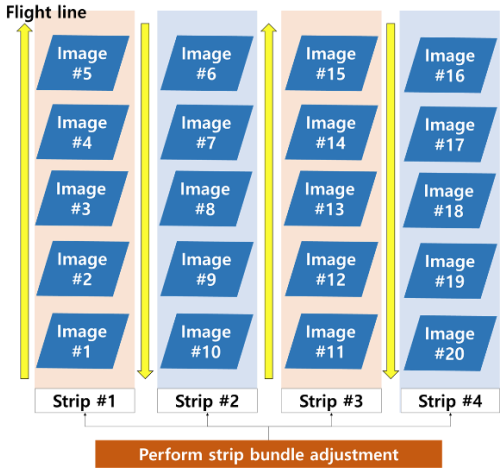

Figure 6. Concept of strip bundle adjustment.

2.3 Extraction of tie-points between adjacent strips

Next, the tie-points were extracted between adjacent strips. This tie-point extraction was different from the tie-point extraction in step 2.1 in that this selected tie-points visible in two sequential images in one strip and one image in the adjacent strip as triplets. Through this, we attempt to extract triplets among image strips. Figure 7 shows the example of triplet points between strips. By considering tie-points from the opposite flight direction, we minimize the misalignment errors that may occur between strips.

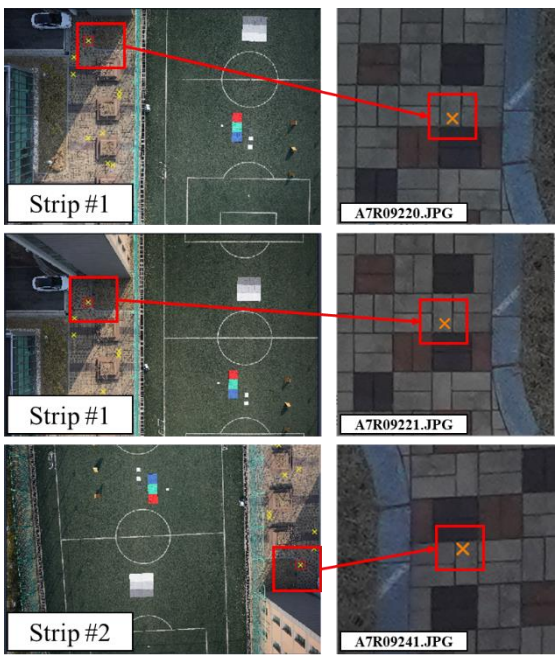

Figure 7. Example of triplet points in inter strip.

2.4 Block bundle adjustment

Block adjustment was performed using all the extracted tie-points in every strip (Figure 8). In this study, the re-weight least square estimation method was used to estimate unknown parameters, and to adjust EOPs (Yoon and Kim, 2022). The adjustment model equation is shown in Eq. 2. In the equation, we tried to select and apply initial weights for reliable parameters. This minimized adjustment for high-accuracy observation data and increased adjustment for uncertain observation data. This made the estimation results more reliable. For example, EOPs were acquired using a GPS/IMU sensor with high precision. Therefore, we could assign greater weights for EOPs , then weights for other parameters. This made the adjustment for the initial EOPs to be minimal. The result of the estimation could be controlled by adjusting the weights for each parameter.

$$\begin{bmatrix} w & 0 & 0 \\ 0 & \dot{w} & 0 \\ 0 & 0 & \ddot{w} \end{bmatrix} \begin{bmatrix} \dot{B} & \ddot{B} \\ I & 0 \\ 0 & I \end{bmatrix} \begin{bmatrix} \dot{\Delta} \\ \ddot{\Delta} \end{bmatrix} = \begin{bmatrix} w & 0 & 0 \\ 0 & \dot{w} & 0 \\ 0 & 0 & \ddot{w} \end{bmatrix} \begin{bmatrix} \epsilon \\ \dot{C} \\ \ddot{C} \end{bmatrix} \quad (2)$$

where $\dot{B}, \ddot{B}$ = coefficients of partial differential equations for EOP and ground coordinates of tie points in collinearity conditions
I = coefficients of identity matrix
$\dot{\Delta}, \ddot{\Delta}$ = increments for EOP and ground coordinates of tie points
ϵ = differences between observed and initial values for collinearity equations
$\dot{C}, \ddot{C}$ = differences between observed and initial values for EOP and ground coordinates of tie points
$w, \dot{w}, \ddot{w}$ = accuracy of collinearity equation, EOPs, tie-points, respectively

We obtained the estimated adjustment values based on the initial weights for each estimation loop. After obtaining the covariance of the estimated solution, the weight factors were calculated. The adjustment loop was determined to be completed if the weight factors converged to 1.

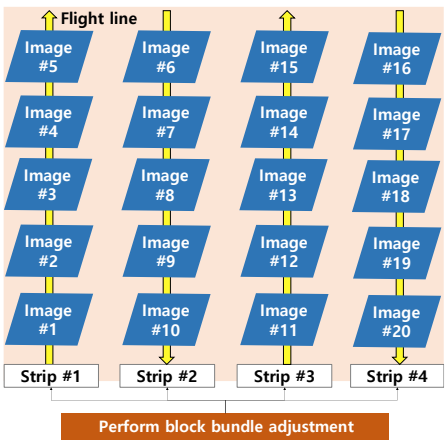

Figure 8. Concept of block bundle adjustment.

2.5 Mosaic image generation

A mosaic image was generated by using adjusted EOPs from the block bundle adjustment. Each image was transformed to a mosaic plane using the estimated EOPs. To observe discrepancies around image boundaries, any image mosaic techniques such as seamline extraction or image blending were not applied.

3. RESULTS AND DISCUSSION

Two types of comparisons were performed. The first comparison was quantitative analysis comparing the true sensor offset values with the estimated sensor offset values through the proposed method. The second comparison was qualitative analysis assessing the presence of misalignment errors between images through the generation of mosaic images.

Table 1 shows the number of tie-points used in each experiment dataset. There were 598 tie-points extracted between strips of the same flight direction, and 682 tie-points were extracted between strips of the opposite direction. Thus, a total of 1280 tie-points were extracted and used throughout the experiment in Dataset 1. Similarly, in Dataset 2, there were 559 tie-points for strip adjustment, and 668 tie-points were extracted for inter strips. Therefore, 1227 tie-points were totally used to estimate the unknown parameters.

Dataset	The number of images	Tie-points along flight lines (same/inter)	Total tie-points
1 (Incheon)	56	598/682	1280
2 (Jeon-Ju)	47	559/668	1227

Table 1. the number of the used tie-points, and image with Datasets1, 2.

Table 2 describes initial weights for each dataset applied in the experiment. The GPS/IMU sensor used in the experiment was the Trimble APX-15 UAV, known for its high level of observation accuracy. Therefore, in all datasets, the initial weight for EOP were set to 1, while the initial weight of tie-point position was set to $1/1e+20$. We confirmed that all datasets were converged within 7-8 loops, using re-weighted LSE. We also confirmed that RMSE (Root mean square error) for result of estimation were 1.16, and 0.89. From this result, it was confirmed that the estimation has been performed stably.

We compared estimated sensor offsets from the proposed method with true sensor offset values. The true values had been estimated using extensive GCPs.

GCP were acquired in the same area with Dataset 2. We estimated true offset values by the method developed for estimating sensor offsets using GCPs in our previous research (Kim et al., 2022). We compared sensor offsets estimated using GCPs only with sensor offsets estimated using tie-points only.

Table 3 shows the result of comparison for sensor offsets using GCPs and tie-points.

We could confirm that the difference between the estimated sensor offsets using GCPs and using tie-points were similar. We could confirm that sensor offsets can be sufficiently estimated even if using tie-points only. In particular, the difference in the average value of the estimated boresight angle of dataset 1 was estimated to be low at 0.092. The difference between the average values of the boresight angle of dataset 2 was 0.373, which was estimated to be relatively higher than that of dataset 1.

Dataset	Sensor offset	Estimated values		
		Tie-points	GCPs	Difference
1	ω (deg)	-0.723	-0.633	0.090
	ρ (deg)	0.343	0.338	0.005
	Κ (deg)	0.278	0.261	0.017
	△WPK			**0.092**
	X_L (m)	0.159	0.117	0.042
	Y_L (m)	0.126	0.027	0.099
	Z_L (m)	1.869	1.272	0.597
	△XYZ			**0.246**
2	ω (deg)	0.656	-0.633	0.023
	ρ (deg)	0.397	0.338	0.059
	Κ (deg)	1.301	0.261	1.040
	△WPK			**0.373**
	X_L (m)	0.159	0.117	0.042
	Y_L (m)	0.174	0.027	0.147
	Z_L (m)	1.409	1.272	0.137
	△XYZ			**0.205**

Table 3. Comparison of estimated sensor offsets using only tie-points and GCPs (Ground Control Points).

Next, we checked the misalignment errors by creating a mosaic image. In Figure 9, we can confirm that the misalignment was adjusted depending on whether the boresight angle and lever-arm offset were applied. The misalignment was gradually improved from the mosaic image. Finally, the mosaic image generated showed an improvement for misalignment in the adjacent images when the boresight angle and lever-arm were simultaneously applied.

Figure 10 shows a comparison of mosaic images with sensor offsets estimated using GCPs and mosaic images with sensor offset estimated using tie-point only. No significant misalignments were observed in the two mosaic images. Thus, we can confirm that the estimated sensor offsets from our proposed method were applied efficiently.

On the other hand, it was observed that misalignment still remained in dataset 2 with the same weight applied in Figure 11(a). This misalignment was thought to be caused by error of the estimated boresight angle in Table 3. Rather, when the sensor offset was estimated by another weight without applying the same weight, it was confirmed that the misalignment in the mosaic image was corrected (Figure 11 (b)).

Dataset	Loop	Miscloser	Initial weights							Y Parallex	RMSE
			Colinear Model	Lever-arm	Boresight angle	EOP (ω,ρ,κ)	EOP (X_s, Y_s, Z_s)	Tie-points (X, Y, Z)	CM		
1	7	9.37e-08	1	$\mathbf{1/1}e$+20	1 * rad	1 * rad	1	$\mathbf{1/1}e$+20	0.00710	1.05	1.16
2	8	5.78e-08	1	$\mathbf{1/1}e$+20	1 * rad	1 * rad	1	$\mathbf{1/1}e$+20	0.00424	0.83	0.89

Table 2. Comparison of initial weights for dataset 1 and 2.

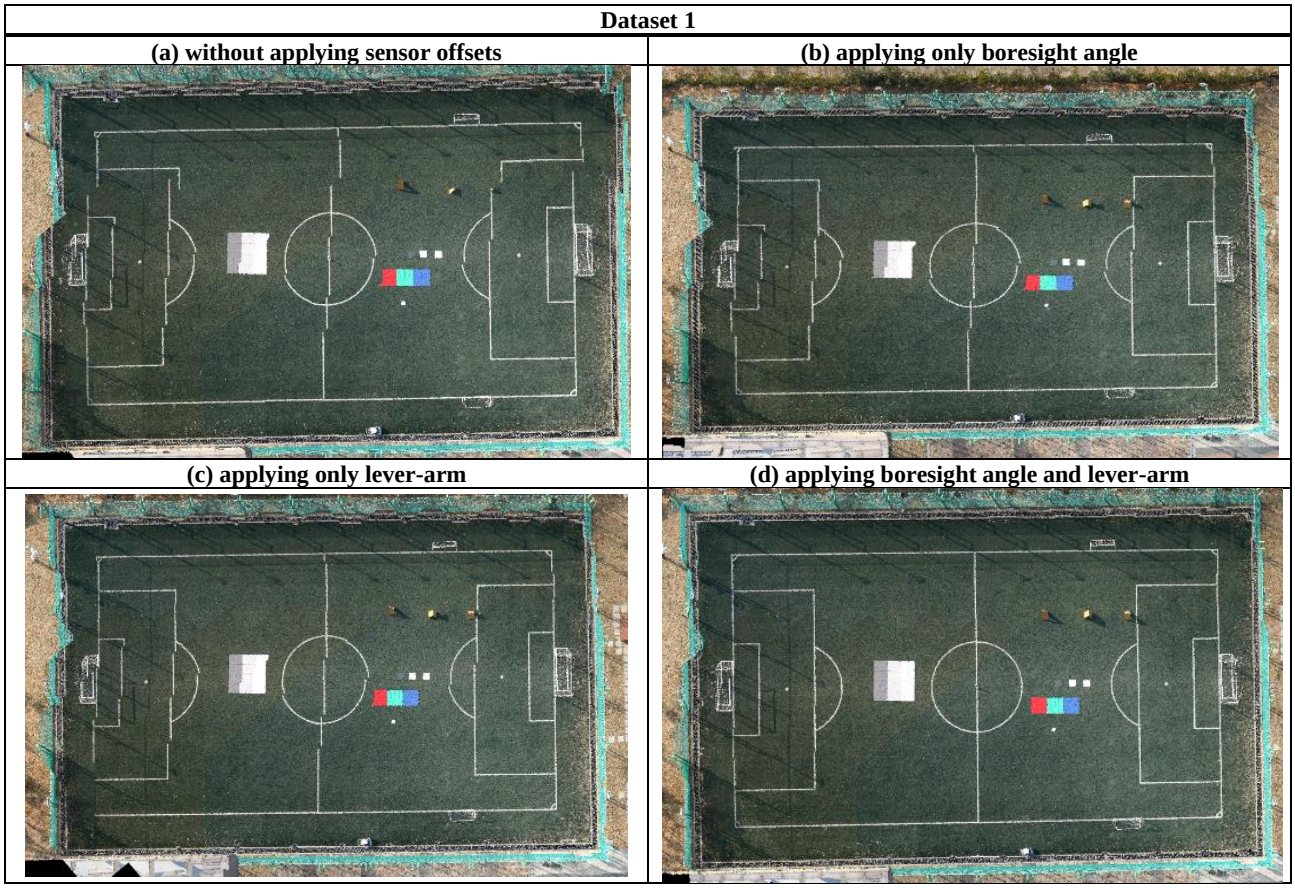

Figure 9. Comparison of mosaic image in Dataset 1 (Korea Polar Research Institute, Incheon)

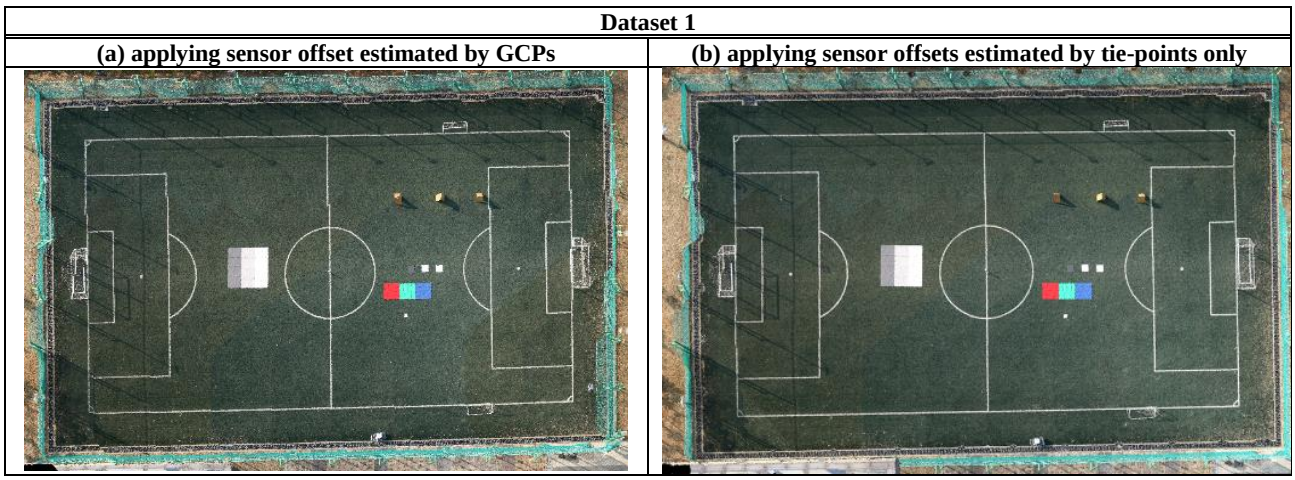

Figure 10. Comparison of mosaic image by sensor offset estimated GCPs and tie-points.

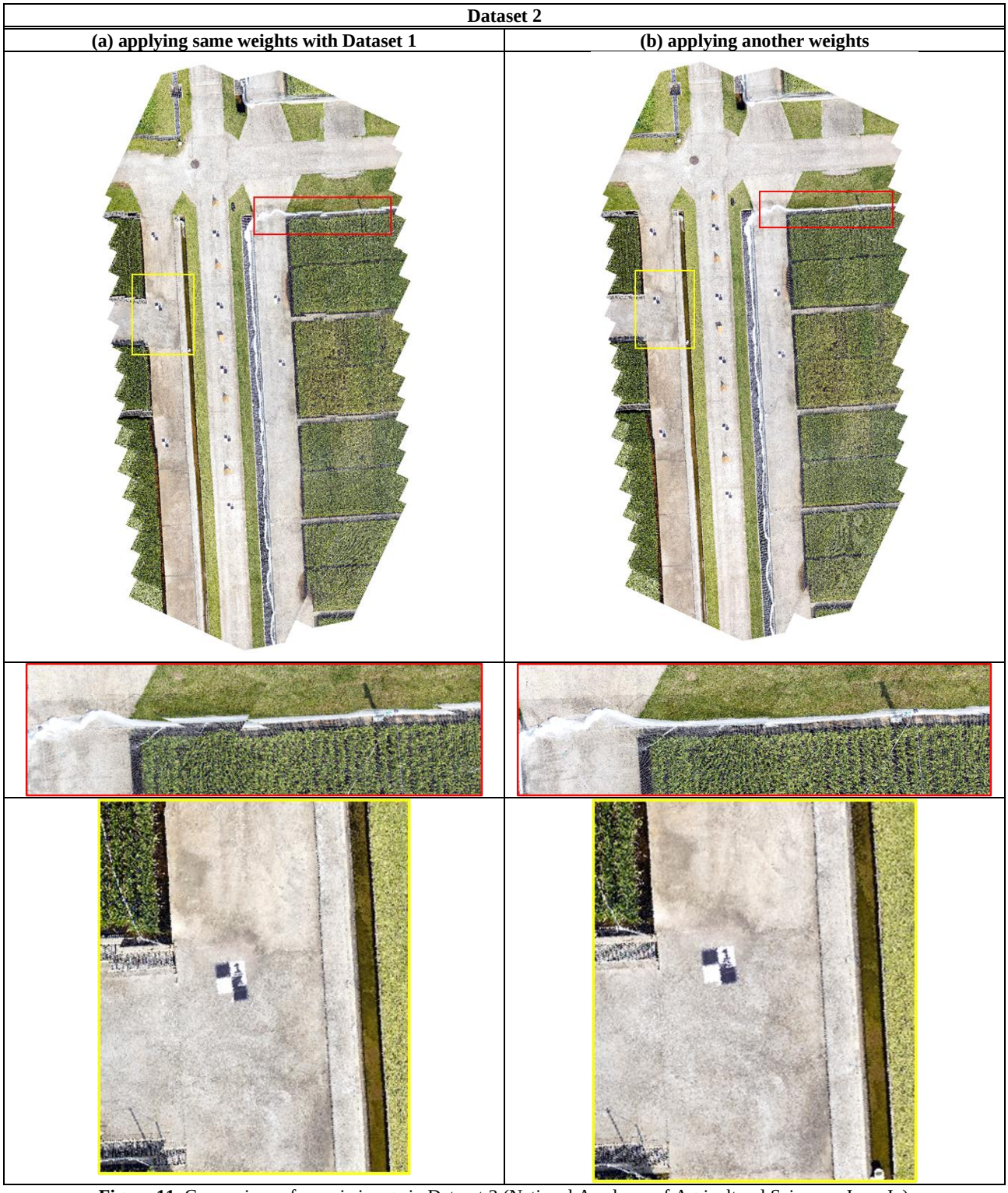

Figure 11. Comparison of mosaic image in Dataset 2 (National Academy of Agricultural Sciences, Jeon-Ju)

4. CONCLUSIONS

Through this study, we were able to confirm several facts. We firstly confirmed that the sensor offset of the platform could be estimated only with the tie-points extracted between adjacent images. We expect that the UAV platform may be free from expensive costs to be paid for sensor offset measurements or from GCP surveys performed on the field to estimate sensor offsets.
We also could confirm that misalignments in the mosaic images were corrected when boresight angle and lever-arm were simultaneously estimated and applied. The corresponding misalignment reduction was checked visually in mosaic images. We can propose that the boresight angle and lever-arm parameter should be considered in the sensor model equation in order to obtain more accurate mosaic images.
We could also confirm that the estimation results could be significantly affected by how the weights for estimation parameters were assigned. The sensor offset estimated from the proper weights produced a mosaic image with corrected misalignment.
On the other hand, we confirmed that misalignment was not adjusted when the weights for dataset1 were applied to dataset 2. This is considered to be the effect of the applied weights. The misalignment errors were reduced when the appropriate weight was applied to dataset2.
In the future research, we will check the effectiveness of the dataset according to the weights, and we will research how to select weights that can be applied generally. We expect that further improvements to the proposed method will enable the flexible operation of UAV platforms.

ACKNOWLEDGEMENTS

This work was supported by Korea Polar Research Institute (KOPRI) grant funded by the Ministry of Oceans and Fisheries (KOPRI PE22910).

REFERENCES

Habib, A., Zhou, T., Masjedi, A., Zhang, Z., Flatt, J.E., and Crawford, M., 2018. Boresight calibration of GNSS/INS-assisted push-broom hyperspectral scanners on UAV platforms, *IEEE Journal of Selected Topics in Applied Earth Observations and Remote Sensing*, 11(5), 1734-1749.

Keyetieu, R., and Seube, N. 2019. Automatic data selection and boresight adjustment of LiDAR systems. *Remote sensing*, 11(9), 1087.

Kim, C. W., Lim, P. C., Chi, J. H., Kim, T., and Rhee, S., 2022. Physical Offset of UAVs Calibration Method for Multi-sensor Fusion. *The Korean Society of Remote Sensing*, 38(6), 1125-1139.

Li, Z., Tan, J., and Liu, H., 2019. Rigorous Boresight Self-Calibration of Mobile and UAV LiDAR Scanning Systems by Strip Adjustment, *Remote Sensing*, 11(4): 442.

Lim, P. C., Rhee, S., Seo, J., Kim, J. I., Chi, J., Lee, S. B., and Kim, T., 2021. An Optimal Image–Selection Algorithm for Large-Scale Stereoscopic Mapping of UAV Images. *Remote Sensing*, 13(11), 2118.

Mittal, P., Singh, R., and Sharma, A. 2020. Deep learning-based object detection in low-altitude UAV datasets: A survey. *Image and Vision computing*, 104, 104046.

Yoon, S., and Kim, T. 2022. Tin-Based Robust Mosaicking of Uav Images with Consecutive Image Connection. *The International Archives of the Photogrammetry, Remote Sensing and Spatial Information Sciences*, 43, 423-430.

Zhang, W., Li, X., Yu, J., Kumar, M., and Mao, Y. 2018. Remote sensing image mosaic technology based on SURF algorithm in agriculture. *EURASIP Journal on Image and Video Processing*, 2018, 1-9.